GAMMA OSCILLATIONS AND COUPLING IN PRIMATE HIPPOCAMPUS DURING SLEEP

Gamma Oscillations and Their Cross-frequency Coupling in the Primate Hippocampus during Sleep

Saori Takeuchi, BA[1,5]; Tatsuya Mima, MD, PhD[2]; Rie Murai, MMedSc[1]; Hideki Shimazu, MD, PhD[3]; Yoshikazu Isomura, MD, PhD[4]; Toru Tsujimoto, MD, PhD[1,5]

[1]Supportive Center for Brain Research, National Institute for Physiological Sciences, Okazaki, Japan; [2]Human Brain Research Center, Kyoto University Graduate School of Medicine, Shogoin, Sakyo-ku, Kyoto, Japan; [3]McGovern Institute for Brain Research, Massachusetts Institute of Technology, Cambridge, MA; [4]Tamagawa University Brain Science Institute, Tokyo 194-8610, Japan; [5]The Graduate University for Advanced Studies (SOKENDAI), Shonan Village, Hayama, Kanagawa, Japan

Study Objectives: The mechanism by which sleep consolidates memory is unclear. Based on the two-stage model of memory consolidation, different functions for slow wave sleep (SWS) and rapid eye movement (REM) sleep have been proposed; thus, state-dependent changes of neural oscillations in the hippocampus might clarify this fundamental question.

Methods: We recorded hippocampal local field potentials from freely behaving monkeys via telemetry and analyzed their nonstationary oscillations using Hilbert-Huang transform.

Results: By applying a recently developed empirical mode decomposition analysis, we found strong cross-frequency coupling between high-frequency and slow wave oscillations during SWS and a prominent increase of gamma band activity in short bursts during REM sleep in unanesthetized primates' hippocampus.

Conclusion: Spatiotemporal integration through coupled oscillations during slow wave sleep might be a physiological basis of system consolidation, whereas gamma bursts during rapid eye movement sleep might be related to synaptic consolidation in the local hippocampal neural circuit.

Keywords: cross-frequency coupling, Hilbert-Huang transform, hippocampus, monkey, REM sleep

Citation: Takeuchi S, Mima T, Murai R, Shimazu H, Isomura Y, Tsujimoto T. Gamma oscillations and their cross-frequency coupling in the primate hippocampus during sleep. *SLEEP* 2015;38(7):1085–1091.

INTRODUCTION

Oscillations are universal phenomena in the brain and their synchrony is thought to be relevant for the interregional communication and integration in the framework of cell assembly hypothesis.[1,2] Particularly, the gamma band oscillation might enable information coding as well as learning and memory formation through spike-timing-dependent plasticity.[3,4] Furthermore, recent studies revealed the interaction between different frequency bands. Indeed, the slow wave oscillation modulates the gamma band activity, which might be a physiological basis of complex cognitive operations.[4–6] This cross-frequency coupling (CFC) might be associated with the long-range synchronization of local gamma networks, thus facilitating the spatiotemporal integration of multiple cell assemblies.[3,7,8]

State-dependent changes of neural oscillations have been extensively studied.[3,9] Among various aspects of sleep, memory consolidation during sleep has been extensively discussed in the field of neuroscience. Regarding the functional difference between rapid eye movement (REM) sleep and slow wave sleep (SWS, stages 3 and 4), the sequential hypothesis of the two-stage model of memory consolidation was proposed recently.[10] In this framework, SWS achieves the integration of new memory into long-term memory network (system consolidation), whereas REM sleep strengthens the long-term memory representation (synaptic consolidation).

Submitted for publication June, 2014
Submitted in final revised form December, 2014
Accepted for publication December, 2014
Address correspondence to: Toru Tsujimoto, MD, PhD, National Institute for Physiological Sciences, Okazaki, 444-8585, Japan; Tel: +81-564-55-7799; Fax: +81-564-52-7913; Email: tujimoto@nips.ac.jp

Because this functional difference in sleep stages is likely to be reflected in the organization of hippocampal oscillations, we hypothesized that CFC would be stronger during SWS to enable system consolidation via spatiotemporal integration of two memory stores and that neural synchrony would be larger during REM sleep to facilitate synaptic consolidation through spike-timing-dependent plasticity. To test this hypothesis, we investigated the spectral property and CFC of local field potential (LFP) oscillations in the hippocampus of three freely behaving monkeys (ML, MO, and MP) during natural sleep (Figure 1A–1C). Sleep stages were defined by a standard method identical to that used in human sleep studies.[11]

Because we expect that LFP oscillations are generated by dynamic and nonlinear neural systems, Hilbert–Huang transform (HHT) was used to characterize their frequency properties.[12] HHT is an adaptive data analysis method that uses empirical mode decomposition, and it can detect the instantaneous phase, frequency, and amplitude of nonlinear and nonstationary processes without *a priori* defined functions.[13]

METHODS

Three adult Japanese monkeys (weight, 6–8 kg; two females, ML and MO; and one male, MP) were used in this study. The protocol was approved by the institutional ethics committee of the National Institute of Natural Sciences. All experimental procedures were conducted in accordance with the National Research Council/Institutes for Laboratory Animal Research Guide for the Care and Use of Laboratory Animals. The current data sets were recorded as a part of a larger study protocol for other purposes.

Recording

The hippocampal electrodes were inserted from the occipital aspect through the parasagittal plane to the lateral (L) and

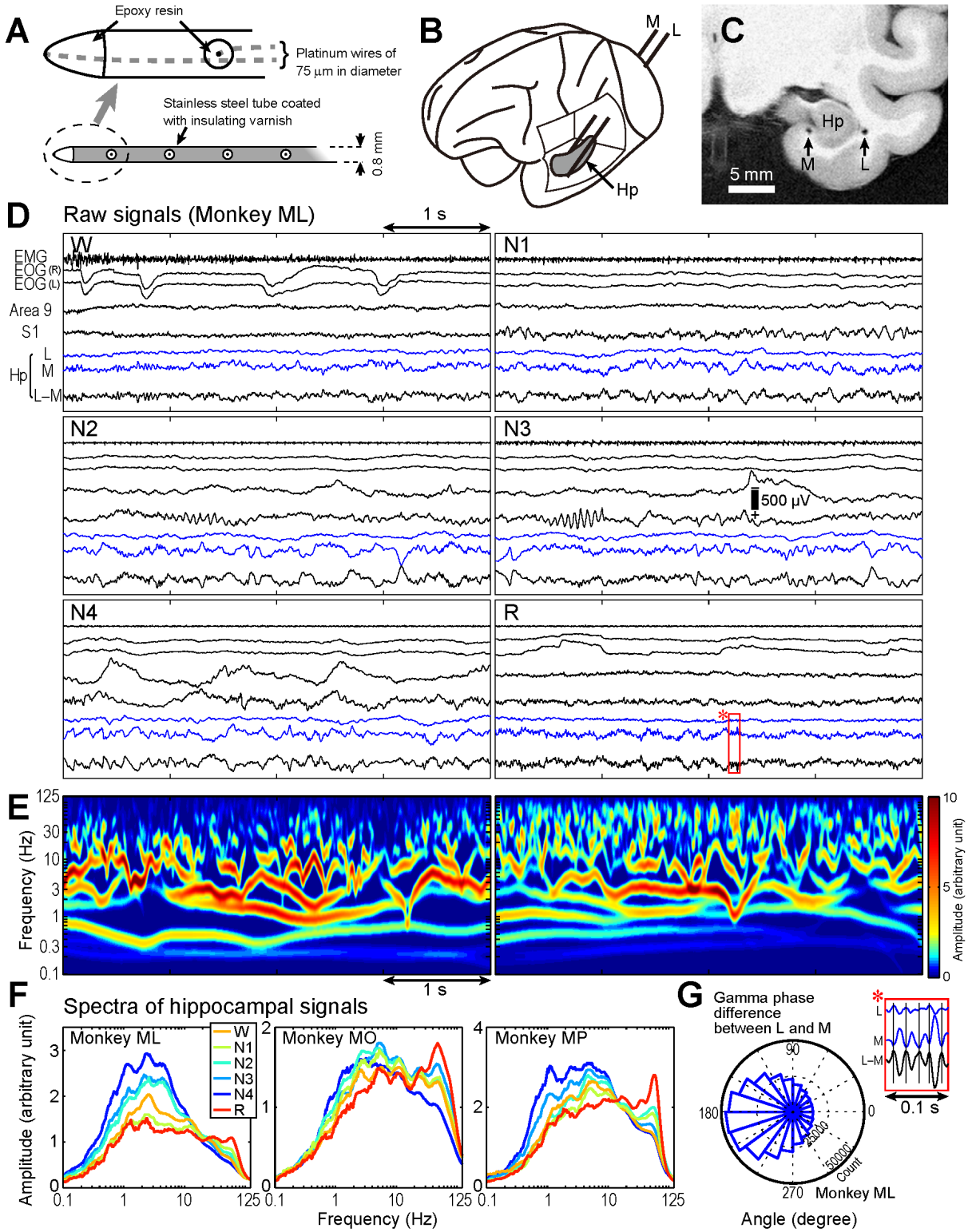

Figure 1—Hippocampal recording procedure and hippocampal local field potential (LFP) during sleep. **(A)** Schematic illustrations of hippocampal electrodes. **(B)** Locations of lateral (L) and medial (M) electrodes. **(C)** Postmortem magnetic resonance image of monkey ML. **(D)** Example raw data traces for the L–M potential (Hp) with electromyogram (EMG), electrooculogram (EOG), and neocortical LFPs recorded from prefrontal and primary sensory areas (areas 9 and S1) during wakefulness (W), non-rapid eye movement (non-REM) sleep stages 1–4 (N1–4), and REM sleep (R). **(E)** Time-frequency map of the same signal during N4 (left) and REM sleep (right). **(F)** Hippocampal LFP spectra during each sleep stage. **(G)** Hippocampal signal magnifications (marked with a red rectangle in **D**, stage R) and the histogram of gamma phase difference between the L and M signals. Sinusoidal waves at approximately 50 Hz appeared in opposite polarities between L and M. The circular histogram displays gamma oscillations phase angles of L as referenced by M measured at L–M gamma oscillations peaks. Mean angle was 189.3 ± 0.4° (mean ± 2 standard deviations) and was in anti-phase from 90° to 270°. Phase reversal between L and M was also confirmed for MO (159.2 ± 0.6°) and MP (208.9 ± 0.3°). These results indicate that the current sources of characteristic gamma oscillations were likely in the hippocampus between the L and M electrodes.

medial (M) surface of the hippocampus along its longitudinal axis (L and M electrodes, Figure 1A and 1B). The hippocampal electrodes comprised a bundle of platinum wires (diameter, 75 μm) with four or seven contacts separated from each other by 4 mm (center-to-center) placed in a 0.8-mm-diameter stainless steel tube coated with insulating varnish (Figure 1A). The electrode impedance was maintained at 2–3 MΩ. The hippocampal LFP was recorded from a pair of L and M electrodes (Figure 1B). Control electrodes were placed in the bone marrow behind the ear on both sides. The control electrodes were connected together and were used as a reference. Additionally, for sleep stage classification, the LFP of multiple cortical regions, electrooculogram (EOG), and electromyogram (EMG) from the posterior neck muscles were recorded. The EOG electrodes were placed superolaterally in the bone marrow of the orbit. After a recovery period of > 1 mo, recordings were performed.

Recordings were performed on freely behaving monkeys in individual cages together with infrared video monitoring using a custom-made telemetry system (time constant: 1 sec, high-cut filter: 200 Hz, A/D rate: 500 Hz, 16 channels). For each monkey, data during 1 night were subjected to the analysis.

The differential L−M potential was used for hippocampal LFP evaluation, as the electrodes were deliberately placed to measure the electrical gradient along the lateral-medial direction. The electrical gradient was produced by the synchronous activation of apical dendrites at the location.[14,15] Raw signals of monopolar L and M potentials and bipolar L−M potentials are shown (Figure 1D; Figure S1, supplemental material). The paired electrodes were deliberately arranged to record the dipole component of electric gradient within the hippocampus along the lateral-medial direction, so that the L and M signals showed the antiphase relationship (Figure 1G). Although the exact generator mechanism of LFP oscillations within the hippocampal structure cannot be determined, we successfully and stably recorded the hippocampal activity of freely behaving monkeys using this large-scale LFP method with minimal surgical damage to the hippocampus. The exact locations of electrodes were confirmed by postmortem magnetic resonance imaging (Figure 1C).

First, sleep stages were determined for epochs of every 20 sec using the neocortical LFP, EOG, and EMG in a standard manner.[11] Then, the simultaneously recorded hippocampal LFPs were segmented and classified into wakefulness (W), rapid eye movement (REM) sleep (R), and non-REM sleep (N1, N2, N3, and N4) stages.

Analysis

For frequency-domain analysis, we applied HHT consisting of two parts: empirical mode decomposition and Hilbert transform.[12,13] Unlike short-time Fourier or wavelet transform, HHT is based on Hilbert transform, and thus, the instantaneous phase, frequency, and amplitude of nonlinear and nonstationary data can be estimated with good temporal and frequency resolution. However, because Hilbert transform can be practically applied to a monocomponent signal within a narrow frequency range, the original signal was decomposed using the empirical mode decomposition in HHT that is an adaptive data-driven method with an *a posteriori* defined basis.[12,13] The only assumption is that any signal consists of different intrinsic modes of oscillations that have the same number of extrema and zero-crossings and is symmetric with respect to the local mean.

Although narrow band-pass filtering has been widely used as preprocessing for Hilbert transform, *a priori*-based linear processing may distort waveforms of the original signal when it is not exactly sinusoidal.

Briefly, all the local extrema are identified, all the local maxima are connected by a cubic spline curve, and the same process is repeated for the local minima. The first component is the difference between the original signal and the mean of the upper and lower envelopes as determined by the aforementioned method. By repeating this decomposition to this first component, the second component is derived. During these repeated procedures, the riding waves are eliminated, making the decomposed component more symmetric with respect to the local mean until it reaches the stoppage criterion (S-number: 5). Consequently, the first intrinsic mode function (IMF), containing the fastest frequency component, is computed. Then, this first IMF is subtracted from the original signal, and the aforementioned procedure is repeated to decompose the second IMF. The procedure is stopped when the residual signal reaches a degree of monotonicity and smallness that precludes further IMF extraction. After this empirical mode decomposition is finished, Hilbert transform is applied to each IMF component to calculate instantaneous phase, frequency, and amplitude. Because the instantaneous frequency is defined through a differentiation procedure in HHT, more data points are needed to define the frequency accurately, as compared to Fourier analysis in which the Nyquist frequency is defined by two points per wave.[12] The minimum number of the data points to define a frequency is empirically known as five (or $4\Delta t$)[12] (the upper limit is 125 Hz when the sampling rate is 500 Hz).

For the time-frequency color map representation of the Hilbert amplitude spectrum as a function of time, the frequency axis was divided into 200 logarithmic bins from 0.1 to 125 Hz. Then, a gaussian filter (full width half maximum: 10 bin × 20 ms) was applied to the map for presentation purposes only.[13] The amplitude spectrum of LFP was computed for each sleep stage by using the marginal mean of amplitudes for each 20-sec segment of LFP. The LFP amplitude of each frequency band during each sleep stage was averaged and normalized to the mean band amplitude of 1 night (delta: 1–4 Hz; theta: 4–8 Hz; alpha: 8–12 Hz; beta: 12–30 Hz; and gamma: 30–80 Hz). To statistically analyze the state-dependent change of LFP amplitude, two-way analysis of variance using frequency and stage as the main factors were performed, followed by Scheffe test. Statistical significance was set at $P < 0.05$.

To measure the burst duration of delta, theta, and gamma activities, the thresholds for burst detection were set to be the mean amplitudes for each frequency band during REM sleep.[16] The duration was measured for each segment continuously exceeding this threshold.

CFC of hippocampal LFP was investigated between the gamma band oscillation and slow rhythms (delta and theta bands). First, to evaluate the amplitude-amplitude CFC, the state-dependent change of linear correlation between the mean amplitudes of gamma band oscillations and those of slow-oscillation waves averaged for each 20-sec epoch were computed for each stage.

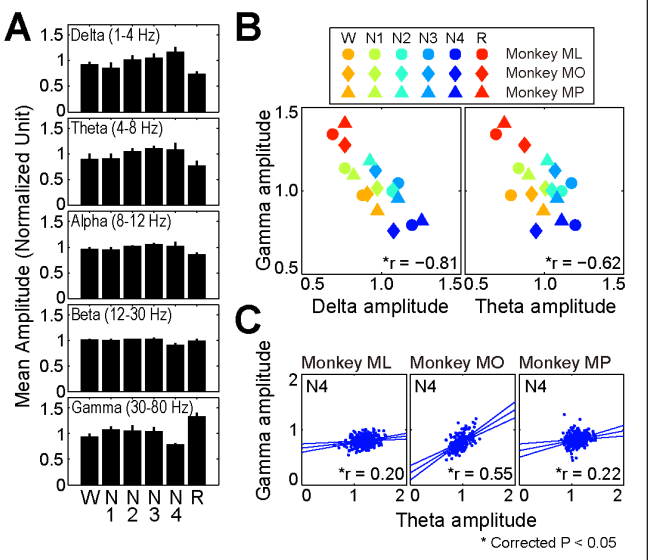

Figure 2—Alteration of band amplitudes during sleep stages. **(A)** The mean amplitude of each band amplitude as a function of sleep stages. The delta/theta amplitude is larger during slow wave sleep (N3 and N4), whereas the gamma band amplitude is larger during rapid eye movement sleep. The error bar represents standard deviation. **(B)** Significant negative correlations between the mean amplitudes of gamma and delta/theta oscillations across sleep stages. **(C)** Within stage N4, the amplitudes of gamma and theta oscillations were positively correlated with each other. The three lines represent the regression line (center) and their 95% confidence intervals (corrected).

Second, to delineate the phase-amplitude CFC, the instantaneous amplitudes of gamma bands were aligned to the trough of slow-oscillation waves and averaged for each sleep stage. Slow-oscillation waves with a duration of > 1 cycle were used for analysis. The amplitudes of gamma bands were normalized to the Z-score using randomly shuffled same data sets.

RESULTS

The dynamic and nonlinear nature of oscillations in multiple frequency bands in the hippocampal LFP (Figure 1D and Figure S1A and S1B; for comparison with wavelet or Fourier transforms, see Figures S2 and S3A and S3B, supplemental material) was successfully detected and visualized by HHT (Figures 1E and S1A and S1B). Although we could observe slow wave oscillations in the delta and theta range during REM sleep in the original waveforms and amplitude spectra (ML: 2.3 Hz; MO: 2.7 and 5.0 Hz; MP: 2.6 and 5.4 Hz), these oscillations appeared in short bursts without displaying stationary slow wave rhythmicity (Figure 1D–1F, and Figure S3C). The amplitude spectra exhibited multiple peaks at nearly harmonic frequencies across different sleep stages (Figures 1F and S3C). The most striking feature of REM sleep-related changes in primate hippocampal activity was the increase of gamma band oscillations (ML: 57.0 Hz; MO: 47.7 Hz; MP: 57.0 Hz). Current sources of the characteristic gamma oscillations were likely in the hippocampus because the polarities of the waves reversed between the L and M electrodes (Figure 1G). The 95th percentiles of burst duration during REM sleep were in the ranges 1.07–1.33 sec, 0.34–0.38 sec, and 0.06–0.09 sec for delta, theta, and gamma oscillations, respectively (Figure S3D).

Quantitative analysis comparing the spectral amplitude across sleep stages identified an increase in the gamma band oscillation during REM sleep compared with the findings in the other stages (Figure 2A). Two-way analysis of variance revealed a significant interaction between frequency and stage ($P < 0.001$). Thus, we performed *post hoc* tests to evaluate the state-dependent change of the LFP amplitude for each frequency band. Briefly, for the delta and theta oscillations, the amplitudes were significantly smaller during REM sleep and larger during SWS (N3 and N4). The gamma band amplitude during REM sleep was significantly larger than that during other stages.

CFC of hippocampal LFP was investigated between the gamma band oscillation and slow rhythms (delta and theta bands). Initially, a significant negative correlation between the amplitude of the gamma band oscillation and that of slow waves in the overall data sets across different sleep stages was noted for amplitude-amplitude CFC (Figure 2B; gamma and delta/theta: $r = -0.81/-0.62$). Because a cooperative relationship between the gamma oscillations and slow waves would produce a positive correlation, the amplitude-amplitude coupling was further evaluated for each sleep stage. Within each sleep stage, although correlation coefficients between the amplitudes of gamma band and slow wave oscillations were mostly nonsignificant or variable across the three monkeys (Figure S4A and S4B, supplemental material), there was a significant positive correlation between the gamma and theta band amplitudes in stage N4 for all monkeys (Figure 2C; $r = 0.20$, 0.55, and 0.22, respectively). These results indicate that cooperative relationship between the gamma and delta/theta bands might be strongest in stage N4.

To delineate the phase-amplitude CFC, the instantaneous amplitudes of gamma bands were aligned to the trough of slow waves and averaged for each sleep stage. The gamma amplitude was significantly modulated by the phase of delta and theta waves (Figures 3, S5, S6, and S7, supplemental material). In all monkeys, the strength of coupling between the gamma amplitude and the phase of slow oscillations was largest during stage N4.

In addition, because the hippocampal activities might be synchronous over large mediotemporal areas, bipolar recording (L−M potentials) might not be appropriate because of their high spatial sharpening effects. Thus, we analyzed the monopolar recordings with extracephalic references (L and M potentials in Figure 1D) and found essentially the same results (Figure S3C).

DISCUSSION

We applied HHT for the analysis of nonstationary neurophysiological data of primates and found that the primate hippocampal LFP oscillations during REM sleep are characterized by the prominent increase of gamma band oscillations in short bursts but not by the existence of rhythmic continuous theta activities, which is consistent with the recent observation using wavelet and Fourier analyses.[17] Extending previous studies on the state-dependent modulation of CFC in nonprimates,[18,19] we found that LFP oscillations during SWS but not during REM

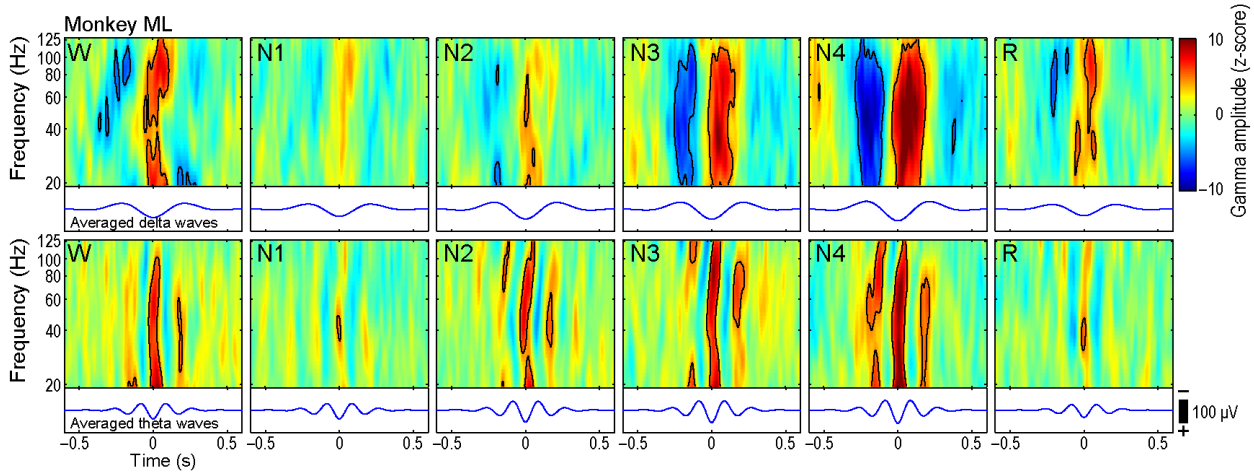

Figure 3—Phase-amplitude cross-frequency coupling (CFC). The mean normalized gamma amplitudes aligned to the trough of delta/theta oscillation. Black contour lines represent the significance threshold at $P < 0.05$ after Bonferroni correction. The most prominent CFC was observed during stage N4.

sleep are characterized by the strong CFC between the gamma band and slow wave oscillations, suggesting the possible activation of system-level network during SWS in primates.

Although some previous studies in nonprimates also noted the existence of gamma band activities during REM sleep, these high-frequency oscillations coexisted with hippocampal rhythmic slow activities (RSA) in the theta range.[20] In studies of humans with epilepsy, some researchers reported the existence of gamma band activities during REM sleep.[21,22] However, most of the studies showed only the slow oscillations in the theta or delta range.[16,23–26] Extending previous studies,[17,21,22] our results showed the increased short bursts of gamma band activities during REM sleep in primates.

In accordance with the recent suggestion that there are species differences in hippocampal RSA,[27] our results showed unique characteristics of monkey hippocampal oscillations during sleep. Gamma oscillations around 50 Hz or higher were most prominently observed during REM sleep, which were not strongly modulated by the phase of slow waves. In contrast, smaller gamma oscillations during SWS were correlated with the phase of slow wave activities. These results indicate the state-dependent modulation of the generator mechanism of gamma oscillations and their CFC with slow waves.

Our observation (Figure 1F) showed that the amplitudes of slow waves increased according to the standard definition of sleep stages.[11] Previous studies in whole night sleeps demonstrated that the delta activities become lower in frequency and smaller in amplitude as the sleep progresses.[28–30] Because we are interested in the difference across sleep stages, this type of whole-night trend in slow wave activities is beyond the scope of the current study.

Gamma band oscillations in cortical LFP might be associated with inhibitory interneuron activities, and they were generated locally within a few millimeters.[31] Their phase-amplitude CFC with slow waves has been implicated as the possible control mechanism for the temporal dynamics and multiregional integration of gamma oscillations.[8,32] An example is the phase-amplitude coupling between the gamma band amplitude and the phase of slow waves, which was first found in the rat hippocampus.[5,33] This coupling has been also reported in the human hippocampus between the delta and gamma bands.[24] Although the cellular basis of this coupling has not been fully elucidated, one plausible mechanism is the entrainment of fast-spiking basket cells into slow waves via an inhibitory network.[5] In accordance with previous studies, the current primate hippocampal study revealed CFC between the gamma band and slow wave oscillations during sleep.

Recent studies suggested the existence of multiple gamma band oscillations, which might represent different physiological mechanisms.[5,6,34,35] In the CA1 region of the rat hippocampus, slow (30–50 Hz), midfrequency (50–90 Hz), and fast (90–150 Hz) gamma bands have been recognized, and they can be differentiated in the different patterns of phase-amplitude CFC.[36,37] In this study, because of the limitation of the telemetric amplifier system (sampling rate: 500 Hz), the very fast gamma oscillation in the range of > 125 Hz could not be reliably analyzed by HHT.[12] Therefore, fast gamma oscillation and hippocampal ripples (approximately 200 Hz)[38] are beyond the scope of our experiment.

In this study, CFC was stronger during SWS even though the absolute amplitude of the gamma band oscillation is larger during REM sleep. This finding indicates the different functions for the gamma band during SWS and REM sleep and fits with the sequential hypothesis of memory consolidation.[10,39,40] The gamma band during SWS might be nested in the slow wave oscillation at the system level, where it may carry the information of the reactivated memory traces, whereas that during REM sleep might be related to the enhancement of synaptic plasticity within the local cell assembly in the hippocampus. Although the results of amplitude-amplitude CFC showed that the amplitudes of gamma band and slow wave oscillations were negatively correlated across sleep stages, a positive correlation in amplitude-amplitude CFC was consistently found during stage N4, suggesting the strong functional link between the gamma band and slow wave oscillations only during SWS.

In the rodent hippocampus, the existence of rhythmic LFP oscillation in the theta range (RSA) is regarded as the signature of REM sleep.[41–46] In addition, the rodent RSA can be observed

during the waking state with exploratory behaviors, despite their apparent behavioral dissimilarity with sleeping.[9,47–49] However, little is known about the characteristics of primate hippocampal oscillations,[17,50,51] and there is considerable debate on the existence of RSA in humans.[16,22–26] A recent review paper suggested that the human hippocampal slow oscillations in patients with epilepsy might be relevant for spatial navigation and memory.[27] These human delta oscillations during REM sleep occur in the medial temporal area[23] or hippocampus[24,25] and can be observed during SWS.[23–25] Moreover, CFC between gamma oscillations and slow activities during REM sleep has been reported.[24] Our results indicated that the slow waves in the monkey hippocampus were irregular in frequency and discontinuous during both REM and non-REM sleep. Although we can find short bursts of slow activities (2–5 Hz) during REM sleep, their amplitudes were larger during non-REM sleep, especially during SWS (Figure 1F). Those slow activities appeared in short bursts of a few cycles (Figure S3D).

Our findings are consistent with the hypothesis that the hippocampal rhythmic slow activity might not be a ubiquitous feature of REM sleep but that its frequency and pattern of occurrence can vary across species.[27] Because the hippocampal activities are often associated with higher cognitive functions in various experimental settings, the large difference between the human and monkey might be possible. The large species differences in hippocampal activities can be partly supported by recent studies in bats.[52,53] Because we only analyzed the primate hippocampal oscillations during sleep, the RSA associated with spatial navigation and memory are beyond the scope of the current study.

Because the RSA in rodents and gamma oscillations in primates are both increased during REM sleep, another hypothesis can be that the gamma band activities in primates might be regarded as the functional analog of rodents' RSA. We speculate that the faster oscillations can handle larger information and memory more precisely with greater processing speed like higher "clock frequency", which should be advantageous for the evolution of intelligence in primates.

ACKNOWLEDGMENTS

The authors thank Dr. H. Toyoda for his assistance with MRI scanning. This study was partly supported by a Grant-in-Aid for Scientific Research (C) 23500471 to Dr. Tsujimoto and for Scientific Research (B) 24300192 to Dr. Mima from the Japan Society for the Promotion of Science.

DISCLOSURE STATEMENT

This was not an industry supported study. The authors have indicated no financial conflicts of interest.

REFERENCES

1. Crick F, Koch C. Some reflections on visual awareness. Cold Spring Harb Symp Quant Biol 1990;55:953–62.
2. Singer W, Gray CM. Visual feature integration and the temporal correlation hypothesis. Annu Rev Neurosci 1995;18:555–86.
3. Buzsaki G, Wang XJ. Mechanisms of gamma oscillations. Annu Rev Neurosci 2012;35:203–25.
4. Fell J, Axmacher N. The role of phase synchronization in memory processes. Nat Rev Neurosci 2011;12:105–18.
5. Bragin A, Jando G, Nadasdy Z, Hetke J, Wise K, Buzsaki G. Gamma (40-100 Hz) oscillation in the hippocampus of the behaving rat. J Neurosci 1995;15:47–60.
6. Tort AB, Kramer MA, Thorn C, et al. Dynamic cross-frequency couplings of local field potential oscillations in rat striatum and hippocampus during performance of a T-maze task. Proc Natl Acad Sci U S A 2008;105:20517–22.
7. Canolty RT, Edwards E, Dalal SS, et al. High gamma power is phase-locked to theta oscillations in human neocortex. Science 2006;313:1626–8.
8. Jensen O, Colgin LL. Cross-frequency coupling between neuronal oscillations. Trends Cogn Sci 2007;11:267–9.
9. Buzsaki G, Moser EI. Memory, navigation and theta rhythm in the hippocampal-entorhinal system. Nat Neurosci 2013;16:130–8.
10. Diekelmann S, Born J. The memory function of sleep. Nat Rev Neurosci 2010;11:114–26.
11. Rechtschaffen A, Kales A. A manual of standardized terminology, techniques, and scoring system for sleep stages of human subjects. Washington, DC: Washington Public Health Service, US Government Printing Office, 1968.
12. Huang NE, Shen Z, Long SR, et al. The empirical mode decomposition and the Hilbert spectrum for nonlinear and non-stationary time series analysis. Proc R Soc A 1998;454:903–95.
13. Huang NE. Introduction to the Hilbert-Huang transform and its related mathematical problems. Interd Math Sci 2005:1–26.
14. Brovelli A, Ding M, Ledberg A, Chen Y, Nakamura R, Bressler SL. Beta oscillations in a large-scale sensorimotor cortical network: directional influences revealed by Granger causality. Proc Natl Acad Sci U S A 2004;101:9849–54.
15. Sasaki K, Gemba H, Hashimoto S. Premovement slow cortical potentials on self-paced hand movements and thalamocortical and corticocortical responses in the monkey. Exp Neurol 1981;72:41–50.
16. Cantero JL, Atienza M, Stickgold R, Kahana MJ, Madsen JR, Kocsis B. Sleep-dependent theta oscillations in the human hippocampus and neocortex. J Neurosci 2003;23:10897–903.
17. Tamura R, Nishida H, Eifuku S, Fushiki H, Watanabe Y, Uchiyama K. Sleep-stage correlates of hippocampal electroencephalogram in primates. PLoS One 2013;8:e82994.
18. Isomura Y, Sirota A, Ozen S, et al. Integration and segregation of activity in entorhinal-hippocampal subregions by neocortical slow oscillations. Neuron 2006;52:871–82.
19. Steriade M, Amzica F, Contreras D. Synchronization of fast (30-40 Hz) spontaneous cortical rhythms during brain activation. J Neurosci 1996;16:392–417.
20. Maloney KJ, Cape EG, Gotman J, Jones BE. High-frequency gamma electroencephalogram activity in association with sleep-wake states and spontaneous behaviors in the rat. Neuroscience 1997;76:541–55.
21. Gross DW, Gotman J. Correlation of high-frequency oscillations with the sleep-wake cycle and cognitive activity in humans. Neuroscience 1999;94:1005–18.
22. Uchida S, Maehara T, Hirai N, Okubo Y, Shimizu H. Cortical oscillations in human medial temporal lobe during wakefulness and all-night sleep. Brain Res 2001;891:7–19.
23. Bodizs R, Kantor S, Szabo G, Szucs A, Eross L, Halasz P. Rhythmic hippocampal slow oscillation characterizes REM sleep in humans. Hippocampus 2001;11:747–53.
24. Clemens Z, Weiss B, Szucs A, Eross L, Rasonyi G, Halasz P. Phase coupling between rhythmic slow activity and gamma characterizes mesiotemporal rapid-eye-movement sleep in humans. Neuroscience 2009;163:388–96.
25. Moroni F, Nobili L, Curcio G, et al. Sleep in the human hippocampus: a stereo-EEG study. PLoS One 2007;2:e867.
26. Moroni F, Nobili L, De Carli F, et al. Slow EEG rhythms and inter-hemispheric synchronization across sleep and wakefulness in the human hippocampus. Neuroimage 2012;60:497–504.
27. Jacobs J. Hippocampal theta oscillations are slower in humans than in rodents: implications for models of spatial navigation and memory. Philos Trans R Soc Lond B Biol Sci 2014;369:20130304.
28. Church MW, March JD, Hibi S, Benson K, Cavness C, Feinberg I. Changes in frequency and amplitude of delta activity during sleep. Electroencephalogr Clin Neurophysiol 1975;39:1–7.

29. Aeschbach D, Dijk DJ, Borbely AA. Dynamics of EEG spindle frequency activity during extended sleep in humans: relationship to slow-wave activity and time of day. Brain Res 1997;748:131–6.
30. Borbely AA, Achermann P. Sleep homeostasis and models of sleep regulation. J Biol Rhythms 1999;14:557–68.
31. Wang XJ, Buzsaki G. Gamma oscillation by synaptic inhibition in a hippocampal interneuronal network model. J Neurosci 1996;16:6402–13.
32. Buzsaki G, Draguhn A. Neuronal oscillations in cortical networks. Science 2004;304:1926–9.
33. Soltesz I, Deschenes M. Low- and high-frequency membrane potential oscillations during theta activity in CA1 and CA3 pyramidal neurons of the rat hippocampus under ketamine-xylazine anesthesia. J Neurophysiol 1993;70:97–116.
34. Colgin LL, Denninger T, Fyhn M, et al. Frequency of gamma oscillations routes flow of information in the hippocampus. Nature 2009;462:353–7.
35. Tort AB, Komorowski R, Eichenbaum H, Kopell N. Measuring phase-amplitude coupling between neuronal oscillations of different frequencies. J Neurophysiol 2010;104:1195–210.
36. Belluscio MA, Mizuseki K, Schmidt R, Kempter R, Buzsaki G. Cross-frequency phase-phase coupling between theta and gamma oscillations in the hippocampus. J Neurosci 2012;32:423–35.
37. Scheffer-Teixeira R, Belchior H, Caixeta FV, Souza BC, Ribeiro S, Tort AB. Theta phase modulates multiple layer-specific oscillations in the CA1 region. Cereb Cortex 2012;22:2404–14.
38. Girardeau G, Zugaro M. Hippocampal ripples and memory consolidation. Curr Opin Neurobiol 2011;21:452–9.
39. Gais S, Plihal W, Wagner U, Born J. Early sleep triggers memory for early visual discrimination skills. Nat Neurosci 2000;3:1335–9.
40. Giuditta A, Ambrosini MV, Montagnese P, et al. The sequential hypothesis of the function of sleep. Behav Brain Res 1995;69:157–66.
41. Buzsaki G, Leung LW, Vanderwolf CH. Cellular bases of hippocampal EEG in the behaving rat. Brain Res 1983;287:139–71.
42. Buzsaki G. Theta oscillations in the hippocampus. Neuron 2002;33:325–40.
43. Green JD, Arduini AA. Hippocampal electrical activity in arousal. J Neurophysiol 1954;17:533–57.
44. Vanderwolf CH. Hippocampal electrical activity and voluntary movement in the rat. Electroencephalogr Clin Neurophysiol 1969;26:407–18.
45. Winson J. Interspecies differences in the occurrence of theta. Behav Biol 1972;7:479–87.
46. Robinson TE. Hippocampal rhythmic slow activity (RSA; theta): a critical analysis of selected studies and discussion of possible species-differences. Brain Res 1980;203:69–101.
47. Ekstrom AD, Caplan JB, Ho E, Shattuck K, Fried I, Kahana MJ. Human hippocampal theta activity during virtual navigation. Hippocampus 2005;15:881–9.
48. Kahana MJ, Sekuler R, Caplan JB, Kirschen M, Madsen JR. Human theta oscillations exhibit task dependence during virtual maze navigation. Nature 1999;399:781–4.
49. Whishaw IQ, Vanderwolf CH. Hippocampal EEG and behavior: changes in amplitude and frequency of RSA (theta rhythm) associated with spontaneous and learned movement patterns in rats and cats. Behav Biol 1973;8:461–84.
50. Skaggs WE, McNaughton BL, Permenter M, et al. EEG sharp waves and sparse ensemble unit activity in the macaque hippocampus. J Neurophysiol 2007;98:898–910.
51. Stewart M, Fox SE. Hippocampal theta activity in monkeys. Brain Res 1991;538:59–63.
52. Heys JG, MacLeod KM, Moss CF, Hasselmo ME. Bat and rat neurons differ in theta-frequency resonance despite similar coding of space. Science 2013;340:363–7.
53. Yartsev MM, Ulanovsky N. Representation of three-dimensional space in the hippocampus of flying bats. Science 2013;340:367–72.

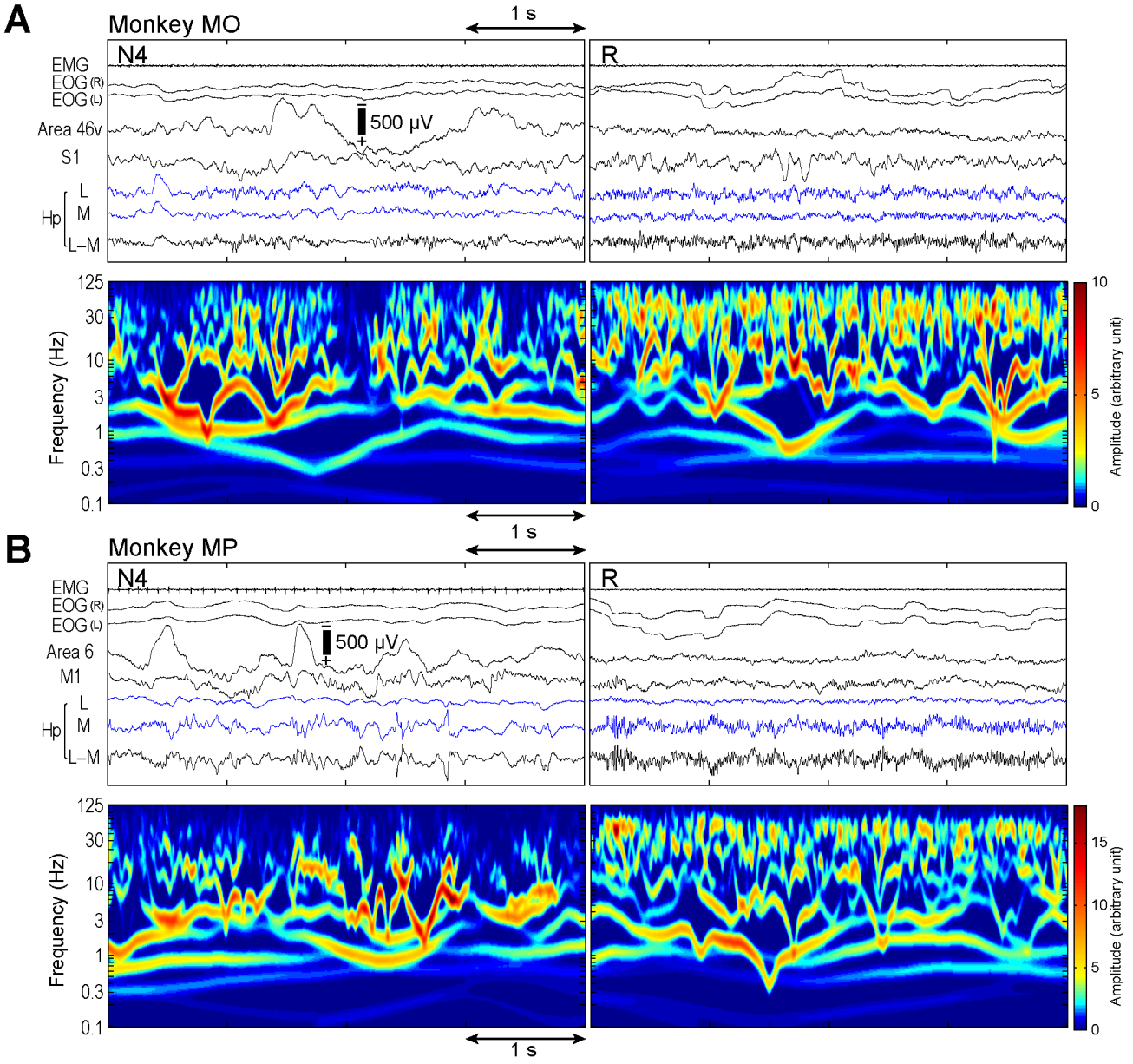

Figure S1—Hippocampal local field potential (LFP) during the sleep of monkeys. (**A**, **B**, upper panels) Example raw data traces for the lateral-medial (L−M) potential (Hp) with electromyograms (EMG), electrooculograms (EOG), and neocortical LFPs recorded from the prefrontal and primary sensory areas (areas 46v and S1) for monkey MO and from the premotor and primary motor areas (areas 6 and M1) for monkey MP during non-rapid eye movement (non-REM), sleep stage 4 (N4), and REM sleep (R). (**A**, **B**, lower panels) Time-frequency map of same signal during N4 (left) and REM sleep (right) computed by Hilbert–Huang transform. For both monkeys, LFP oscillations during REM sleep were characterized by frequent bursts of gamma band activities.

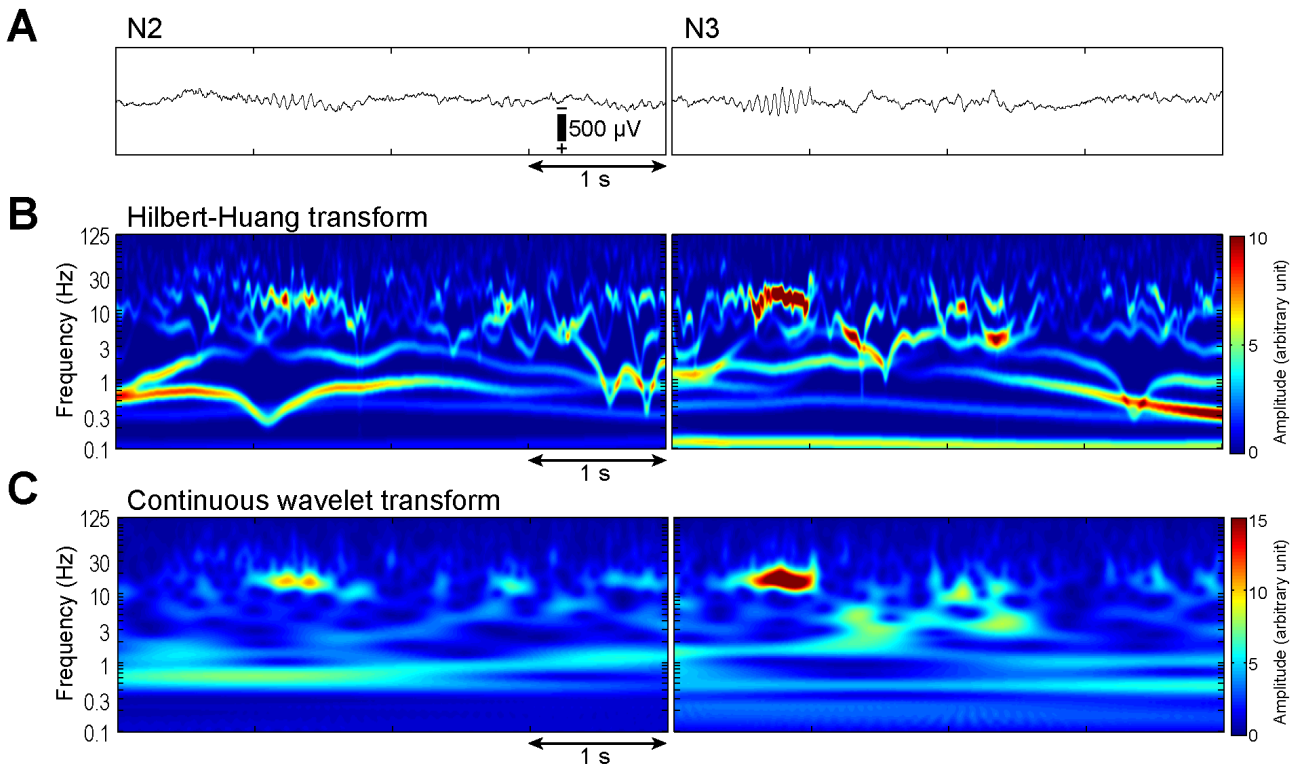

Figure S2—Comparison of Hilbert–Huang transform (HHT) and wavelet analysis. **(A)** Example raw data of spindles in the transcortical potential recorded from the primary somatosensory cortex during stages N2 and N3 (the same data as Figure 1D). **(B)** Time-frequency map of the same signal computed by HHT. **(C)** Time-frequency map of the same signal computed by continuous wavelet transform using complex Morlet wavelet. For both methods, the spindle bursts are clearly depicted. For HHT, the time-varying or dynamic nature of oscillations is demonstrated in detail.

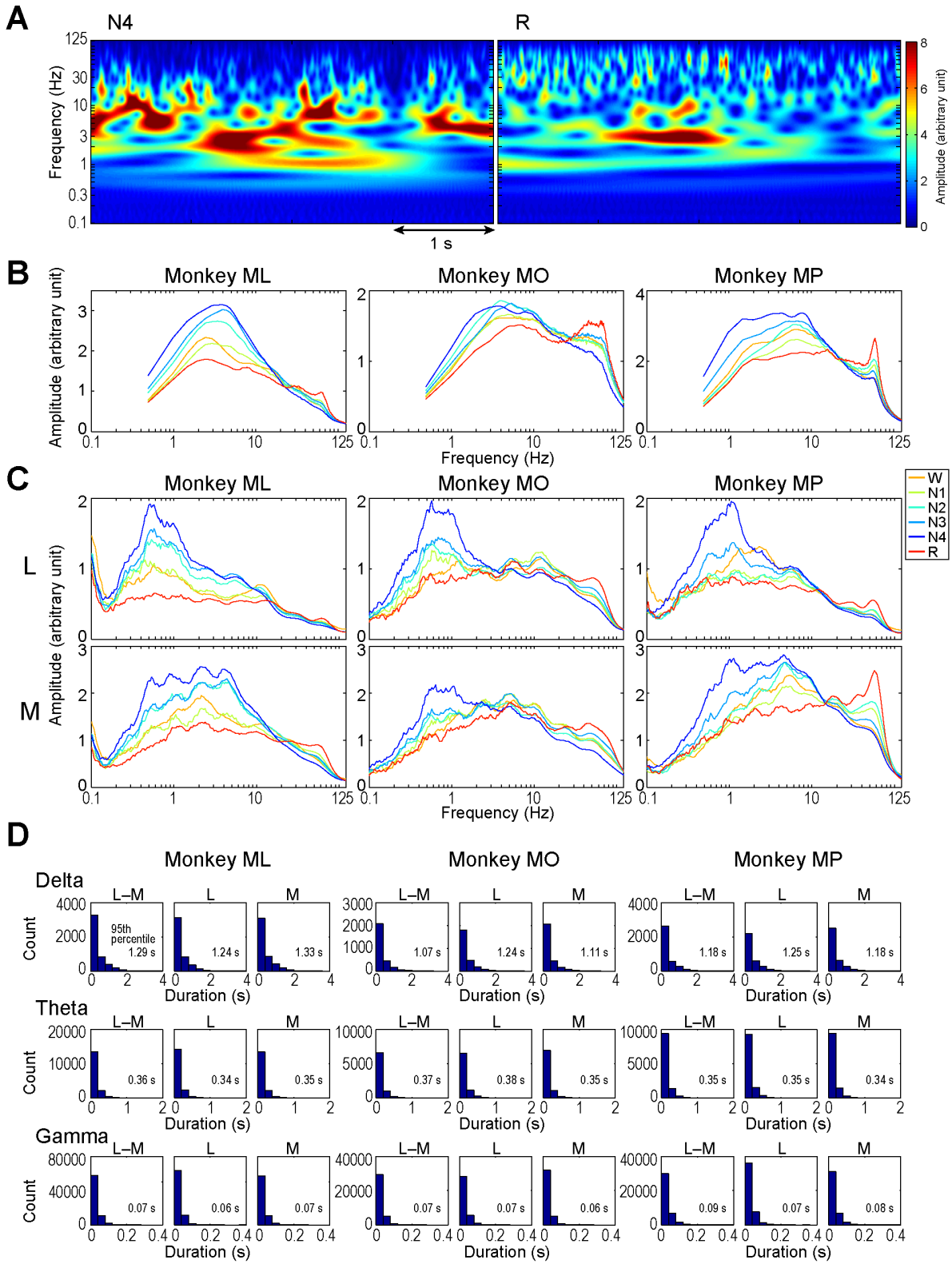

Figure S3—**(A)** Time-frequency map of the same signal as Figure 1E computed by continuous wavelet transform using complex Morlet wavelet. Hilbert–Huang transform (HHT) can detect the nonstationary time-varying patterns of oscillations. **(B)** Hippocampal local field potential (LFP) spectra during each sleep stage computed by short-time Fourier transform using the Welch method (1024 point, frequency resolution: 0.49 Hz). The data set is the same as in Figure 1F. The spectra computed by Fourier method is essentially similar but more smoothed, compared to those computed by HHT. **(C)** Hippocampal LFP spectra during each sleep stage for the monopolar lateral (L) and medial (M) potentials computed by HHT. Monopolar electrodes were referenced to the extracephalic electrodes (the linked bone marrow behind the ear on both sides). The spectra are not very different from those of Figure 1F. **(D)** Histograms of the burst durations of delta, theta, and gamma oscillations during rapid eye movement sleep. Numeric values are the 95th percentiles of the duration.

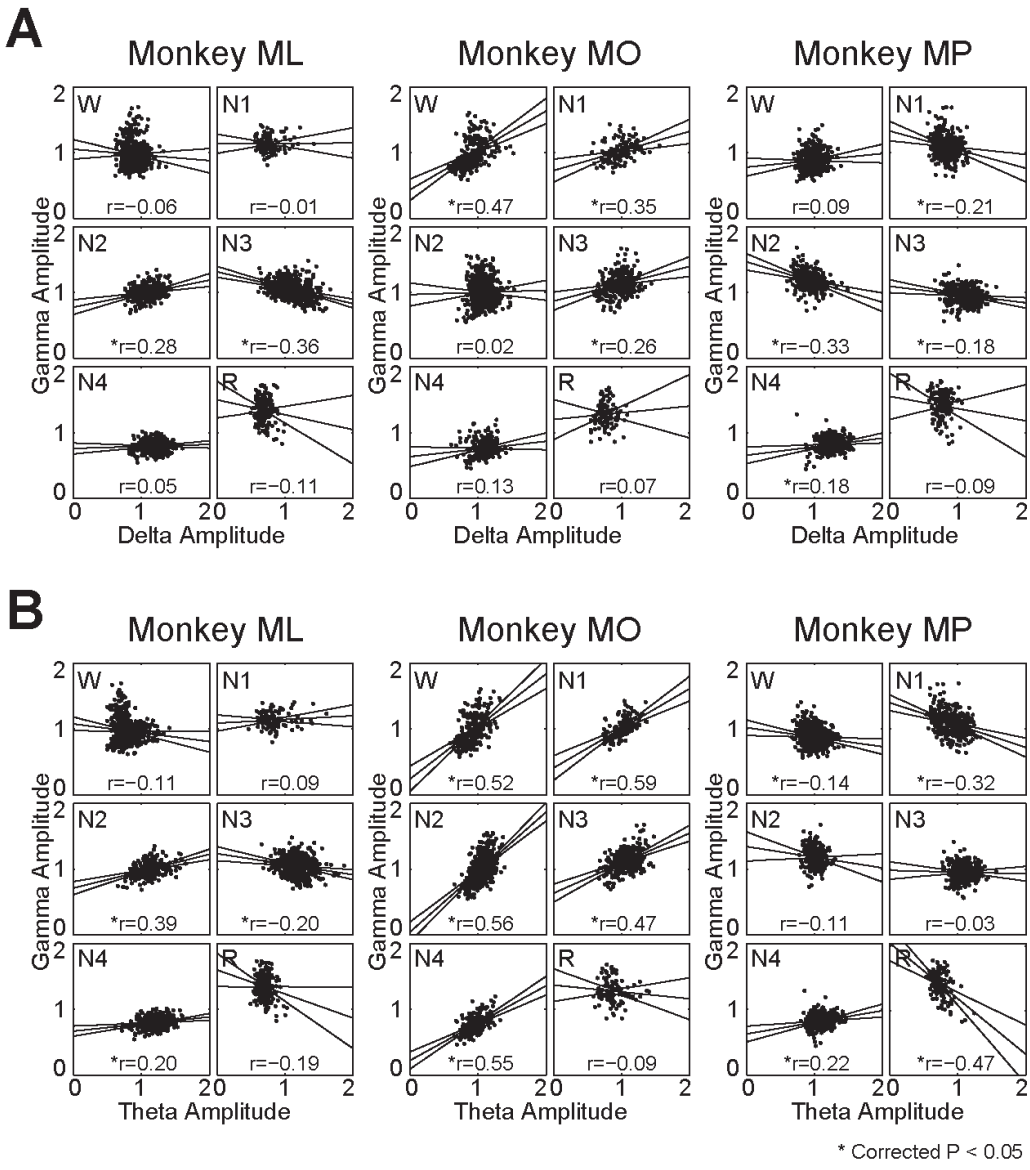

Figure S4—(A) Alterations of band amplitudes during all sleep stages. Correlation x-y plots for the gamma and delta band amplitudes revealed variable results across the monkeys. **(B)** Alterations of band amplitudes during all sleep stages for gamma and theta band amplitudes. A significant positive correlation was observed for the delta-gamma pairing during wakefulness (W) (MO), N1 (MO), N2 (ML), N3 (MO), and N4 (MP) and for the theta-gamma pairing during W (MO), N1 (MO), N2 (ML and MO), N3 (MO), and N4 (ML, MO, and MP). A significant negative correlation was observed for the delta-gamma pairing during N1 (MP), N2 (MP), and N3 (ML and MP), and for the theta-gamma pairing during W (MP), N1 (MP), N3 (ML), and R (MP). A positive correlation of the amplitudes for the theta-gamma pairing was consistently found across the monkeys only during stage N4.

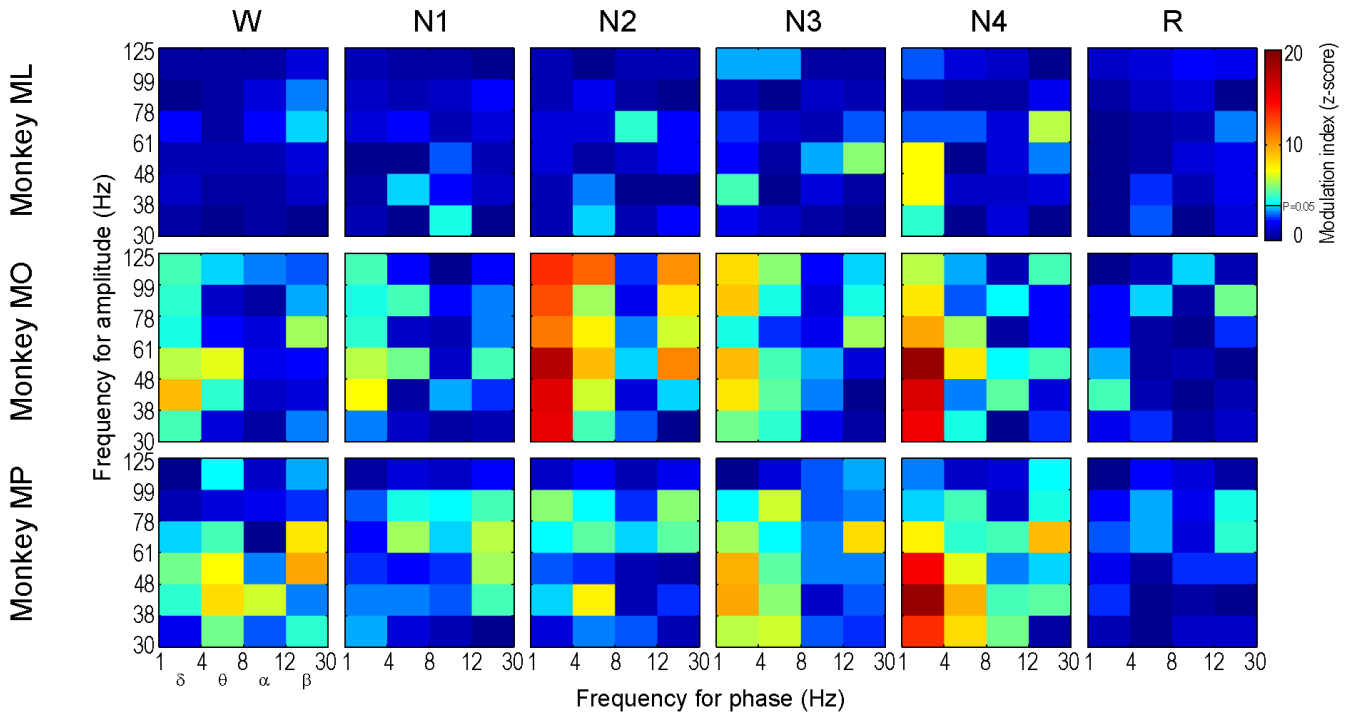

Figure S5—Phase-amplitude cross-frequency coupling (CFC) in all frequencies. As a preliminary analysis to investigate the overall pattern of CFC, the modulation index maps were constructed for three monkeys according to Canolty et al. (2006)[7] using Hilbert–Huang transform. We first computed a composite complex signal by combining the amplitude of the gamma oscillation (30–125 Hz) and the phase of slower oscillation (1–30 Hz). The degree of asymmetry of probability density function of this signal measured by its mean provides an objective index of phase-amplitude coupling. The results are normalized by the surrogate data created by offsetting the gamma and slower oscillations with some random time lag (n = 200). As expected, the results confirmed that the consistent phase-amplitude coupling for the delta and theta frequencies during non-rapid eye movement (non-REM) sleep stages.

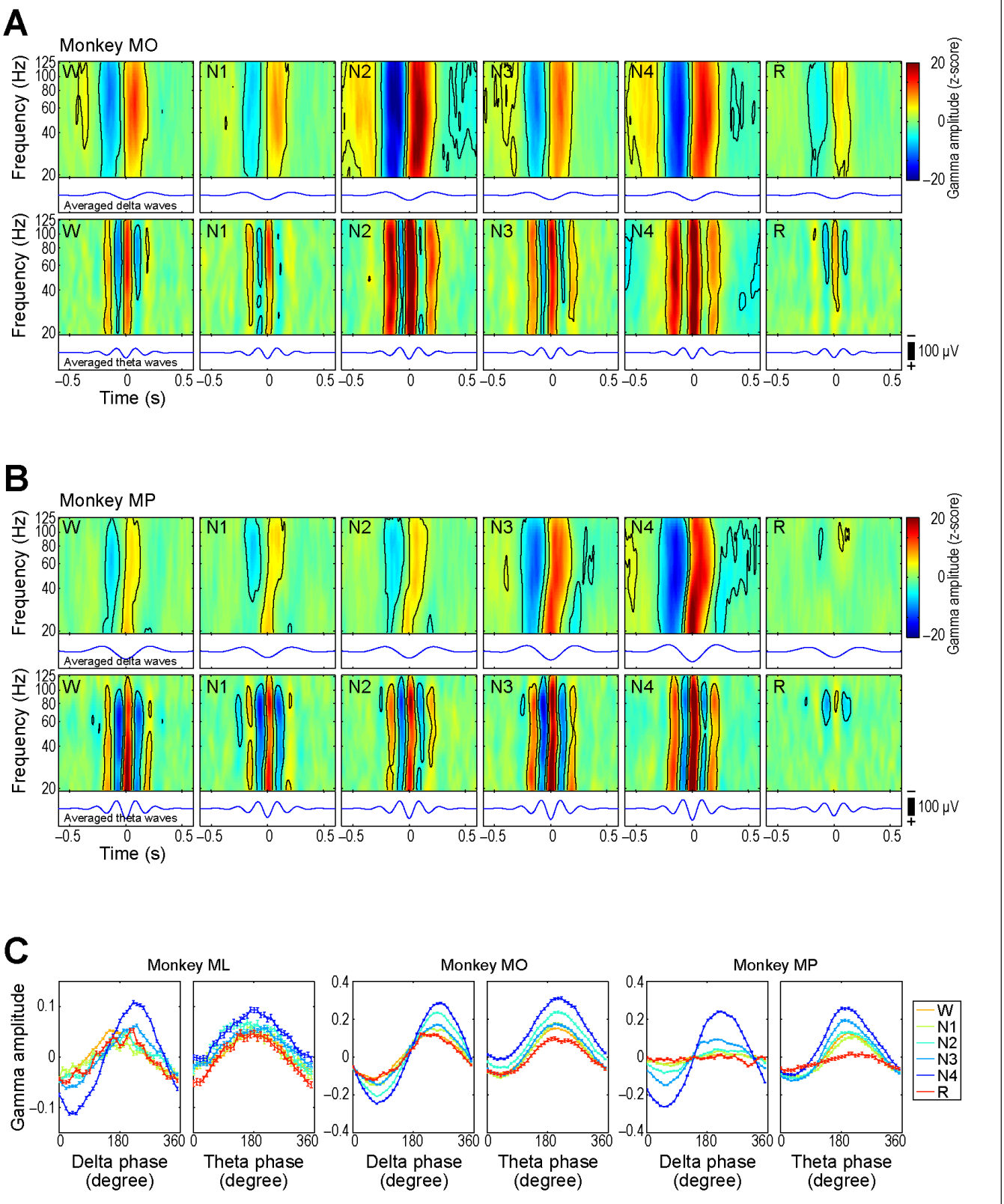

Figure S6—(A,B) Phase-amplitude cross-frequency coupling (CFC) of monkeys. The mean normalized gamma amplitudes aligned to the trough of delta/theta oscillation of monkeys MO and MP. Black contour lines represent the significance threshold at $P < 0.05$ after Bonferroni correction. **(C)** CFC was strongest in stages N2 and N4 of MO and in stage N4 of MP. To investigate the phase relationship between the slow wave oscillation and gamma band amplitude, we plotted the mean gamma band amplitude as a function of phase of the delta/theta waves. The error bar represents standard error. In terms of the phase angle of slow wave oscillations, the occurrence of peak gamma amplitude was variable across monkeys. However, the phase angle corresponding to the peak gamma amplitude was constant across sleep stages in each monkey for delta and theta waves.

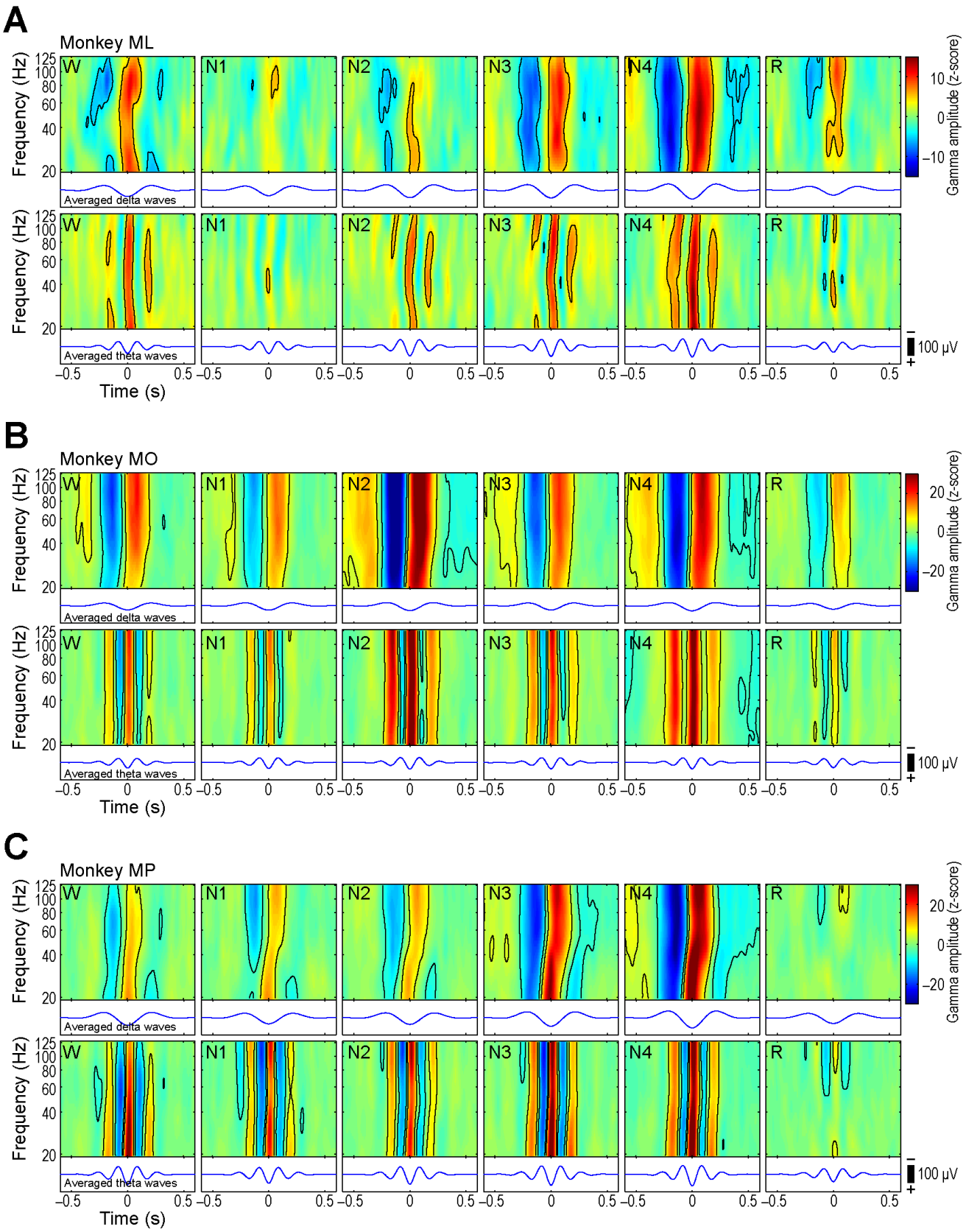

Figure S7—(A–C) Phase-amplitude cross-frequency coupling (CFC) of monkeys computed by continuous wavelet transform using complex Morlet wavelet. The mean normalized gamma amplitudes aligned to the trough of delta/theta oscillation of monkeys ML, MO, and MP. The data sets are the same as in Figures 3 and S6. The pattern is essentially similar for Hilbert–Huang transform and wavelet transform.